Received 19 August 2020; accepted 7 September 2020. Date of publication 11 September 2020; date of current version 4 November 2020.
The review of this article was arranged by Editor A. A. Manaf.

Digital Object Identifier 10.1109/JEDS.2020.3023577

Analysis of Switching Under Fixed Voltage and Fixed Current in Perpendicular STT-MRAM

S. FIORENTINI [1], R. L. DE ORIO [2], S. SELBERHERR [2] (Life Fellow, IEEE), J. ENDER [1], W. GOES [3], AND V. SVERDLOV [1]

1 Christian Doppler Laboratory for Nonvolatile Magnetoresistive Memory and Logic, Institute for Microelectronics, TU Wien, 1040 Vienna, Austria
2 Institute for Microelectronics, TU Wien, 1040 Vienna, Austria
3 Silvaco Europe Ltd., Cambridge PE27 5JL, U.K.

CORRESPONDING AUTHOR: S. FIORENTINI (e-mail: fiorentini@iue.tuwien.ac.at)

This work was supported in part by the Austrian Federal Ministry for Digital and Economic Affairs, in part by the National Foundation for Research, Technology and Development, and in part by the TU Wien Library through Open Access Funding Program.

ABSTRACT In spin-transfer torque magnetoresistive random access memory, the magnetization dynamics of a free layer is usually assumed to be determined by the torque created via a position-independent current density. In circuits, however, it is the voltage, not the current density, which stays fixed during switching. Therefore, the approximate evaluation of the torque based on a fixed current density becomes questionable in modern magnetic tunnel junctions with a tunneling magnetoresistance ratio of about 200%, where the current density across the structure can vary by a factor of three. In this work, we compare the switching times obtained within a fixed voltage assumption with those from the approximate fixed current density assumption. We demonstrate that the assumption of a fixed current can reproduce the correct switching if the current is appropriately adjusted. It is shown that the correction to the current is not universal and depends on various factors such as TMR, temperature, the size of the structure and resistance area.

INDEX TERMS Spin-transfer torque, MRAM, perpendicular magnetization, tunneling magnetoresistance.

I. INTRODUCTION

The latest advancements in the development of computer memory have been based on the down-scaling of semiconductor components. The drawback to down-scaling is an increased power consumption at stand-by, mainly due to leakages. A viable way of reducing the power consumption is the introduction of non-volatility in integrated circuits. Spin-transfer torque magnetoresistive random access memory (STT-MRAM) combines high speed, excellent endurance, low costs, and is thus promising for applications ranging from IoT and automotive applications [1]–[5] to embedded DRAM, and last level caches [6], [7].

In modern MRAM devices, binary information is stored as the relative orientation of the magnetization of the magnetic layers in a magnetic tunnel junction (MTJ). In the parallel (P) orientation the resistance of the structure is lower than in the anti-parallel one (AP), providing a way of discerning between the two states. In STT-MRAM, the switching between the orientations is achieved by passing an electrical current through the MTJ. When the magnetization in the layers does not have the same direction, the spin of the electrons, polarized by the fixed reference layer, aligns almost immediately with the magnetization in the free layer. Due to conservation of the angular momentum, the spin current polarization change is transferred to the magnetization via the exchange interaction. This exchange provides the spin-transfer torque acting on the magnetization of the free layer [8], [9]. If the current is sufficiently strong, the magnetization of the free layer can be switched between the two stable configurations, parallel or anti-parallel, relative to the reference layer.

In micromagnetic modeling of STT switching, the typical simplified approach is to assume that the current density J($\mathbf{r}$, t) is position- and time-independent [10]. In circuits, however, the voltage, rather than the current density, remains fixed during switching. The resistance of the tunnel junction

This work is licensed under a Creative Commons Attribution 4.0 License. For more information, see https://creativecommons.org/licenses/by/4.0/

depends on the relative magnetization alignment of the free and the reference layer, so the current through the structure is not constant during the process. Moreover, as the magnetization of the free layer is not uniform at switching, but depends on the position, so does the local tunneling conductance. The assumption of a constant current density adopted in the description of STT-MRAM switching is violated, especially in advanced MTJs with a tunneling magnetoresistance ratio (TMR) of about 200% and higher [11].

We evaluate the validity of the description with the fixed current density for computing the switching time by comparing the results with switching at a fixed voltage. We also consider an approach in which the total current is fixed, but the current density is determined by the local magnetization alignment and the corresponding local resistance. We show that a correction of the current value allows the fixed current approach to correctly reproduce the switching time distribution obtained using a fixed voltage, and that the correction depends on system parameters such as TMR, temperature, size of the structure and resistance area. The present work is an extension to what we previously reported in [12].

II. MODEL

The key element of any modern MRAM cell is an MTJ. It consists of two ferromagnetic layers separated by a thin tunnel barrier. The use of an in-plane CoFeB/MgO/CoFeB MTJ provides a TMR of up to 600% [13]. The TMR is defined as

$$\mathrm{TMR} = \frac{R_{AP} - R_P}{R_P}, \tag{1}$$

where R_P (R_{AP}) is the resistance in the P (AP) MTJ state. A high TMR value is important to reliably discern between the P and the AP configuration.

Due to the interface-induced perpendicular anisotropy, thin layers of CoFeB on MgO are perpendicularly magnetized. In this configuration, the switching path and the thermal relaxation paths for the magnetization coincide, leading to lower switching currents as compared to in-plane magnetized structures [14].

When the current flows through the structure, only the free layer is allowed to switch, while the reference layer must be fixed. This is usually achieved by antiferromagnetic exchange coupling to a second pinned layer [15].

The magnetization dynamics of the free layer can be described by the Landau-Lifshitz-Gilbert (LLG) equation. With the STT torque $\mathbf{T_S}$ added, the LLG equation reads as [10], [16]

$$\frac{\partial \mathbf{m}}{\partial t} = -\gamma\mu_0 \mathbf{m} \times \mathbf{H}_{\mathrm{eff}} + \alpha \mathbf{m} \times \frac{\partial \mathbf{m}}{\partial t} + \frac{1}{M_S}\mathbf{T_S} \tag{2a}$$

$$\mathbf{T_S} = \gamma \frac{\hbar}{2e} \frac{0.5 J_C P_{RL}}{\mathrm{d}(1 + P_{RL}P_{FL}\cos\theta)} \mathbf{m} \times (\mathbf{m} \times \mathbf{x}), \tag{2b}$$

where $\mathbf{m} = \mathbf{M}/M_\mathrm{S}$ is the position-dependent normalized magnetization in the free layer, M_S is the saturation magnetization, α is the Gilbert damping constant, γ is the gyromagnetic ratio, μ_0 is the vacuum permeability, $\hbar$ is the reduced Plank constant, e is the electron charge, J_C is the current density, d is the thickness of the free ferromagnetic layer, θ is the angle between the local magnetization vectors in the free and fixed layer, and $\mathbf{x}$ is the unit vector along the fixed layer magnetization. The effective magnetic field $\mathbf{H}_{\mathrm{eff}}$ includes the external field, the magnetic anisotropy field, the Ampere field, the demagnetizing field, and the stray field from the reference layer/magnetic stack. To model the switching at finite temperature, $\mathbf{H}_{\mathrm{eff}}$ also includes a thermally fluctuating stochastic magnetic field. P_{RL} and P_{FL} are the spin current polarizing factors of the reference and free layer, respectively. In this article, we assume $P_{RL} = P_{FL}$. The relation between polarizing factors and TMR is described after [16] with

$$\mathrm{TMR} = \frac{2P_{RL}P_{FL}}{1 - P_{RL}P_{FL}}. \tag{3}$$

The standard approach to simulate STT switching is to assume a position-independent current density J_C [10]. This assumption can be justified for low values of the TMR, when the resistance difference between P and AP configurations is small. However, modern perpendicularly magnetized MTJs (p-MTJs) possess a large TMR of typically around 200% [11]. In this case the simplified description offered by (2b) is not accurate. When current is flowing, the local magnetization vectors along the free layer are not collinear. This results in a position-dependent current density, which in turn leads to position-dependent spin currents and spin torques.

To evaluate the behavior of the current in a scenario with non-uniform magnetization in the free layer, we compute the current density flowing through the MTJ structure as

$$\mathbf{J_C} = -\sigma \nabla V. \tag{4}$$

The electric potential V in the ferromagnetic contacts is found by solving the Laplace equation.

$$-\nabla^2 V = 0 \tag{5}$$

The conductivity σ is assumed to be constant in the ferromagnetic layers. The local conductance of the barrier is taken as suggested in [9],

$$G(\theta) = \frac{G_P + G_{AP}}{2}\left(1 + \left(\frac{\mathrm{TMR}}{2 + \mathrm{TMR}}\right)\cos\theta\right), \tag{6}$$

and is imposed by Neumann boundary conditions at the interface between the oxide and the ferromagnetic layer.

In Fig. 1b we show the current density for the magnetization configuration snapshot reported in Fig. 1a. The current density is highly inhomogeneous to accommodate the varying conductance across the barrier.

As the fixed voltage leads to a non-uniform current density distribution, the impact of assuming a fixed voltage in switching simulations must be evaluated. We compare switching times obtained within the approach with a *fixed*

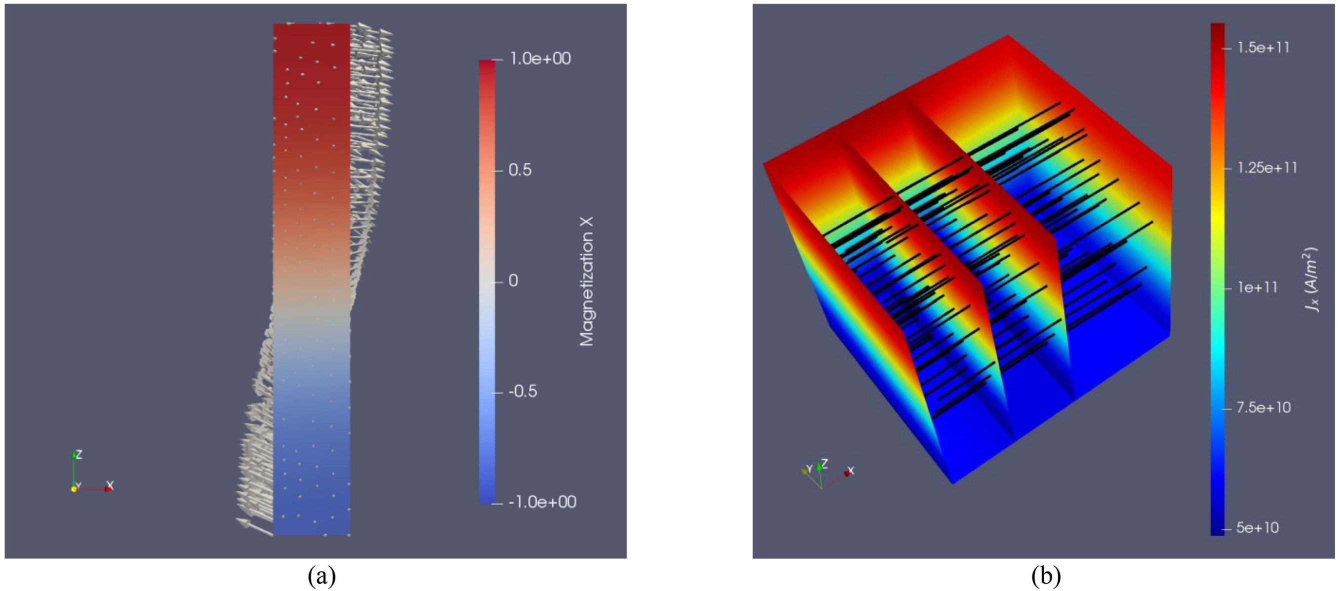

FIGURE 1. (a) Snapshot of the magnetization in the free layer during switching. The magnetization in the fixed layer points along the x direction, so the alignment goes from antiparallel to parallel along the z axis. (b) x-component (perpendicular) of the current density computed in the whole structure. Its value is higher for aligned magnetizations due to lower resistance.

voltage across the MTJ and the one with *constant current density* described by (2) to the reference model [17] generalized to p-MTJs, in which the *total current* is fixed but *redistributed* over time according to the local resistance value. The simulations are performed for a p-MTJ, and the system's parameters are set to typical experimental values ([18], [19]) and are reported in Table 1. The stack is of a pillar shape of 40 nm diameter. The equivalent thicknesses of the free and the reference CoFeB layers are 1.7 nm and 1 nm, respectively. The thickness of the MgO layer is 1 nm. The simulations were performed using the finite-difference method, with a cell size 2 x 2 x 1.7 nm^3.

The expression for the currents in the fixed voltage approach is

$$V = const,\ \ J_C(\mathbf{r}, t) = \frac{G(\theta(\mathbf{r}, t))V}{S},\ \ I(t) = \int dS\, J_C(\mathbf{r}, t), \tag{7}$$

in the fixed current density approach it is

$$J_C = const,\ \ I = J_C S, \tag{8}$$

and in the fixed current approach it is

$$I = const,\ \ J_C(\mathbf{r}, t) = \frac{G(\theta(\mathbf{r}, t))I}{\int dS\, G(\theta(\mathbf{r}, t))}, \tag{9}$$

where I is the total current and S is the surface area of the free layer. The fixed current for the last two approaches is chosen as to be equal to the voltage divided by the resistance in the initial P or AP state, $I = V/R_i$.

III. RESULTS

The switching time is evaluated as an average over twenty realizations, as at room temperature its value depends on

TABLE 1. System parameters.

Parameter	Value
Gilbert damping factor, α	0.02
Saturation magnetization, M_S	1.2 x 10^6 A/m
Free layer thickness, d	1.7 nm
Exchange constant, A	1.0 x 10^{-11} J/m
Perpendicular anisotropy, K	0.9 x 10^6 J/m^3
Thermal stability, Δ	67
Voltage, V	2 V
Resistance Area, RA	18 Ωμm^2
Tunnel Magnetoresistance, TMR	200%
Free layer area, S	1260 nm^2

the stochastic magnetic field modeling the magnetization fluctuations. Fig. 2 reports the dependence of the switching times on the stray field from the reference layer. This can be adjusted thanks to the antiferromagnetic coupling of the reference layer to the pinned layer, and is modeled by the saturation magnetization of the combined layers. As shown in the figure, the average switching times assuming a fixed total current or a fixed current density are remarkably similar for both P to AP and AP to P switching. However, the switching for the fixed constant voltage, with its value chosen so that the initial current before the switching is the same, looks quite different [20]. The difference is due to the fact that, when assuming a fixed voltage, the current depends on the varying resistance of the MTJ. In order to compensate the effect of the varying resistance, the current value I under the assumption of a fixed current must be increased by ∼9% for AP to P and decreased by ∼4% for P to AP switching, for a TMR of 200%. Fig. 3 demonstrates that, after correcting the current, the switching times

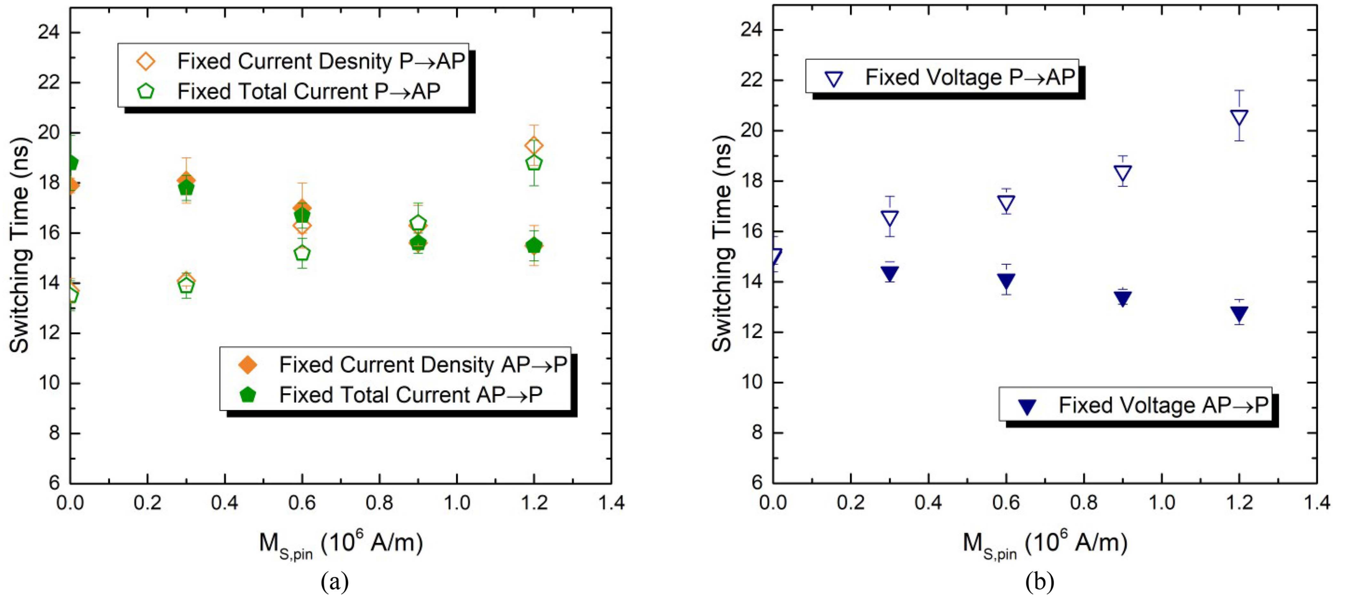

FIGURE 2. Comparison between AP → P and P → AP switching for various levels of the uncompensated stray field at $T = 300$ K. Filled symbols represent AP → P switching, empty ones P → AP. (a) reports the switching times for the fixed current models, (b) the ones for the fixed voltage approach. The bars show switching time variations due to thermal fluctuations.

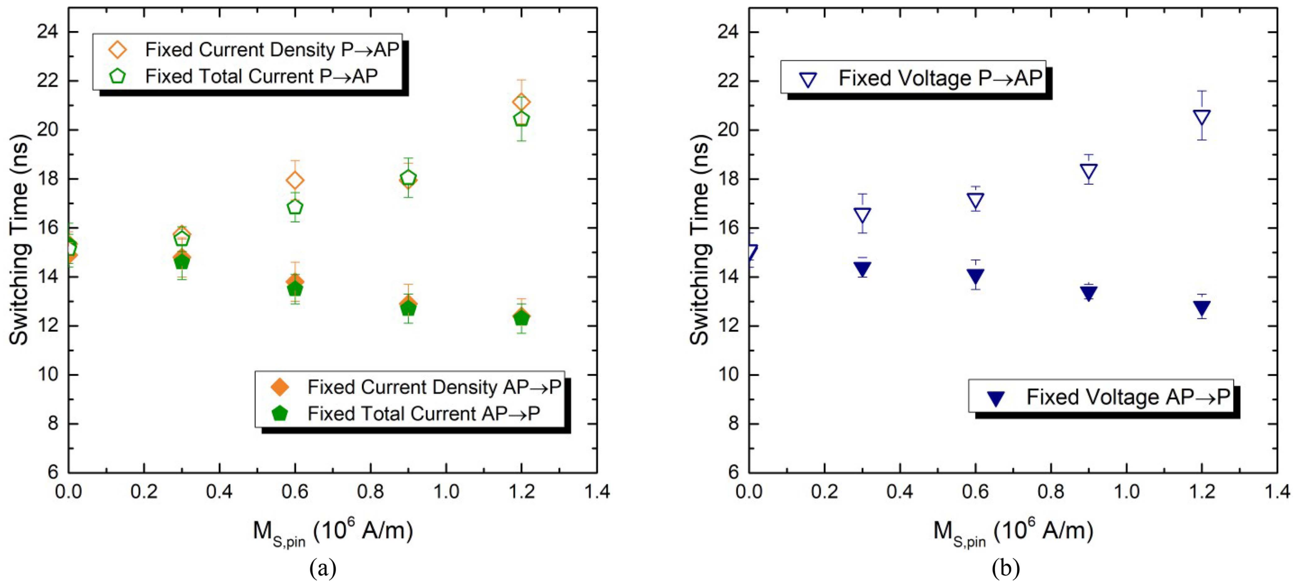

FIGURE 3. Comparison of switching times for the tuned values of input currents at $T = 300$ K. (a) reports the new values for the fixed current models, (b) reports again the switching time at fixed voltage for comparison. The switching times of all three models are compatible within the thermal variation.

as a function of the stray field within the fixed voltage and the fixed current approaches are the same.

We performed simulations of the switching times for various values of the TMR. The dependence on the TMR of the correction, which we had to apply for all the models to produce comparable results, is shown in Fig. 4. The results imply that the constant current density assumption is justified in the realistic case of switching at a constant voltage at *room temperature*, provided that the current is appropriately corrected for the P to AP and the AP to P scenario, and that the correction depends on the TMR.

In order to further elaborate on the origin and magnitude of the current correction, we performed the calculations at zero temperature. Like in the case of room temperature, the results for the switching time under the assumption of a fixed voltage differ from those with the fixed current. However, with the appropriate current correction, all three models provide similar results. The dependence of the correction on the TMR at zero temperature is reported in Fig. 5.

The current correction required is smaller than the one obtained at room temperature. We also note that the switching is faster at room temperature (Fig. 6). This happens

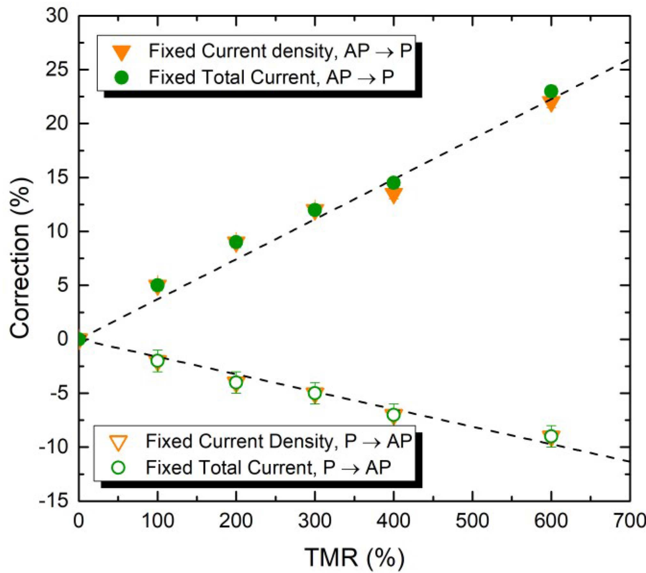

FIGURE 4. **The correction to the current as a function of TMR at $T = 300$ K, which must be given in order for all three models to give consistent results, for both P → AP and AP → P switching. The dashed lines represent a linear fit.**

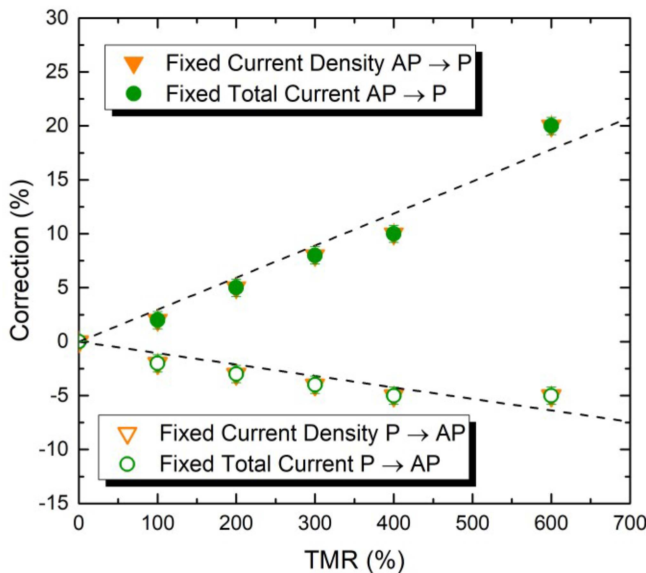

FIGURE 5. **Correction to the current as a function of TMR at $T = 0$ K, for both P → AP and AP → P switching. The dashed lines represent a linear fit.**

because the thermal field helps to move the magnetization from the initial parallel or antiparallel configuration, giving way for the torque to act on it. We investigated the switching time difference between room and zero temperature at various values of the TMR. Results for both AP to P and P to AP switching are reported in Fig. 7. The switching time is always longer at zero temperature than at room temperature. The dependence of the switching time on the TMR can be explained with the help of (2b) and (3). The torque intensity depends directly on the polarizing factor, and thus on the TMR. With higher TMR, the torque is also stronger and so the switching happens faster.

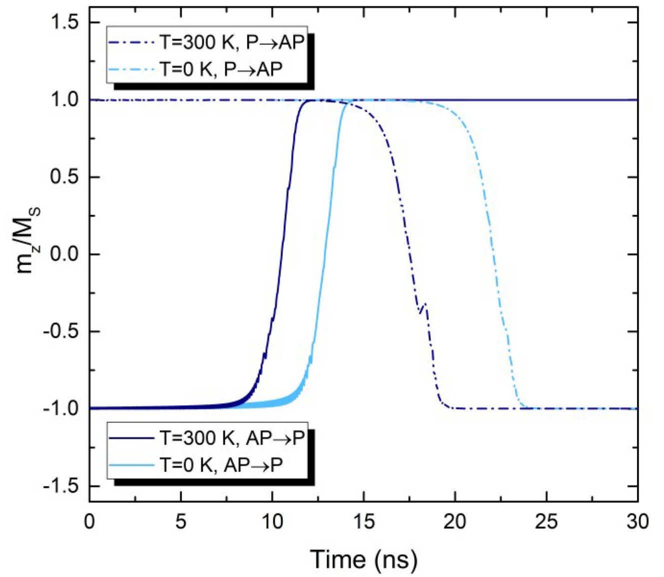

FIGURE 6. **Comparison between switching realizations for the fixed voltage model, with TMR = 200%, at $T = 0$ K and $T = 300$ K. The switching is slower at low temperature.**

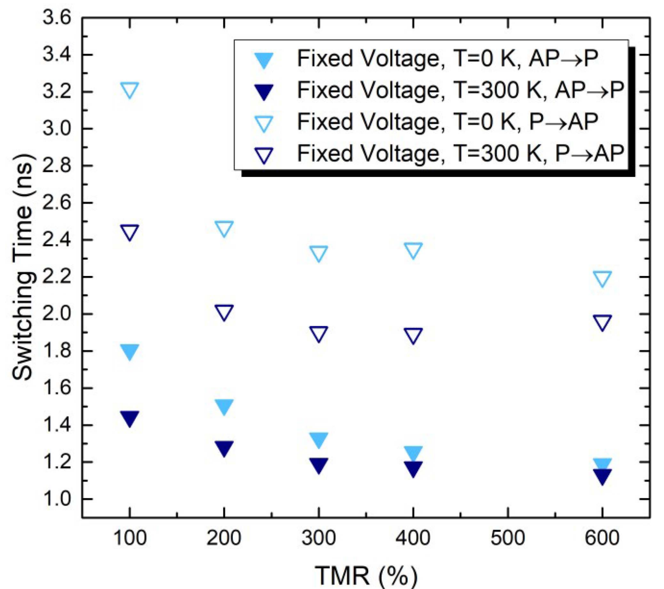

FIGURE 7. **Switching time as a function of the TMR in the fixed voltage approach, for both AP → P and P → AP switching, at $T = 0$ K and $T = 300$ K. The switching time at zero temperature is always higher than the one at room temperature.**

To elaborate on the possible reasons for the dependence of the current correction on the TMR and temperature, we performed macrospin simulations. The simulations were carried out at zero temperature. The initial magnetization direction is slightly tilted from its perfect perpendicular orientation to reduce the incubation time of switching.

Fig. 8 demonstrates that the switching process with a fixed voltage is steeper for AP to P switching than that with a fixed current. In order to compensate for the gradual slope at fixed current, the switching must start earlier, which

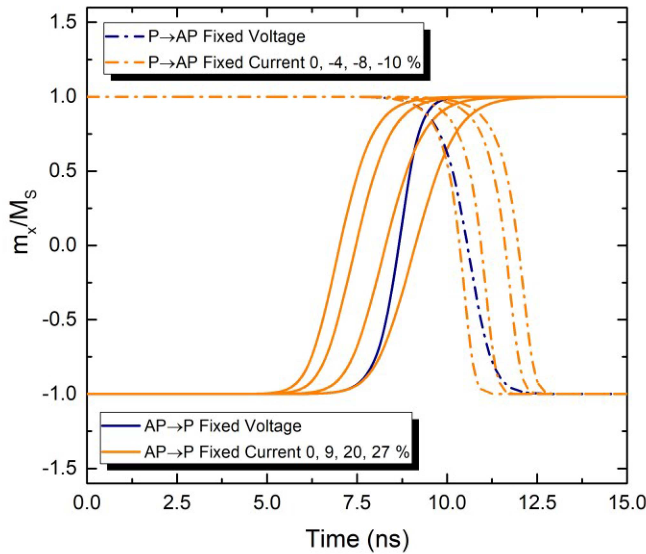

FIGURE 8. Switching realizations in the macrospin scenario for the fixed voltage and fixed current density models, with different values of correction. A higher amount of correction in the fixed current density approach produces faster (slower) switching for AP → P (P → AP). The two approaches present a different slope during switching.

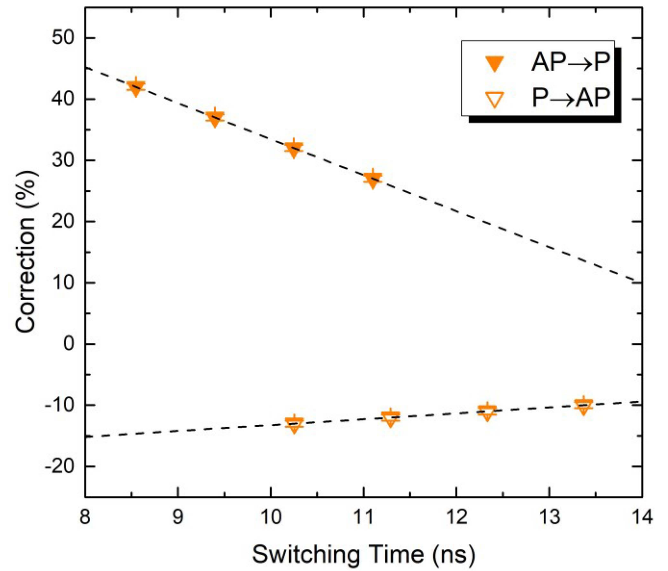

FIGURE 9. Dependence of the correction on the switching time in the macrospin scenario. When the switching becomes faster, a higher amount of correction is required for the fixed current approach to reproduce the switching time of the fixed voltage one.

is achieved by increasing the current. For the switching in the opposite direction the trend is reversed, and the fixed current model provides a steeper switching. Therefore, we need to lower the current to make the switching start later and compensate for the difference in slope by decreasing the current.

We can explain this behavior with the help of equations (1)-(3). In the model with fixed voltage the dependence of the current on the magnetization configuration completely compensates the angular dependence in the denominator of (2b), so the torque magnitude only depends on the sine of the angle between magnetization vectors, coming from the vector product term.

Under the fixed current assumption, the denominator is minimal at the beginning of AP to P switching, when the torque is the same as under the fixed voltage assumption. The denominator becomes larger as the configuration proceeds towards P. This trend must be compensated by a current correction to increase the current. The scenario is opposite for the case of P to AP switching, in agreement with Fig. 8. The denominator is maximal at the beginning and becomes weaker as the configuration proceeds towards AP, and the trend is compensated by a weaker current.

By gradually increasing the initial tilting angle, we can monitor the dependence of the current correction on the switching time, as reported in Fig. 9. The data show that a faster switching requires a higher correction to the current value. As the average switching time is shorter at room temperature, it explains a slightly larger current correction required to match the results for switching times from all three models at $T = 300$ K as compared to the simulations at $T = 0$ K.

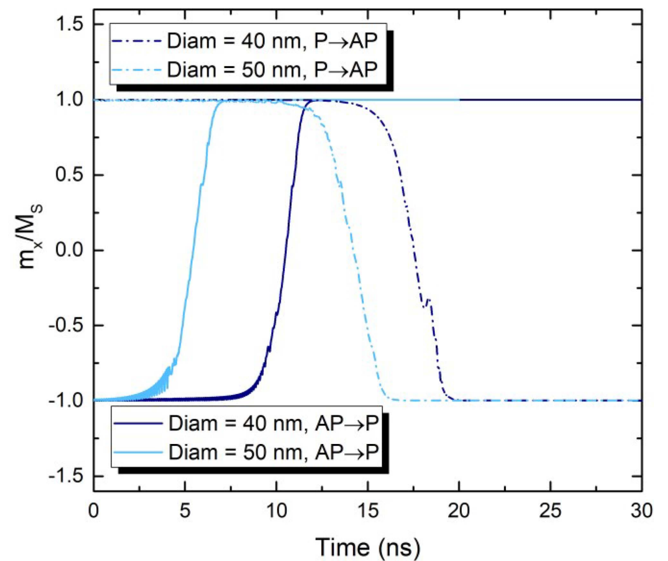

FIGURE 10. Comparison between switching realizations for the fixed voltage model, with TMR = 200% and $T = 300$ K, at diameters of 40 nm and 50 nm. The switching is slower for the smaller structure size.

In order to corroborate these findings, we performed switching simulations with various surface areas. The simulations were performed by keeping the same current density for every choice of area. When the size of the junction is bigger, the resistance is lower, and the total current flowing through the structure is higher. Moreover, it is easier to create subdomains in the magnetization and initiate the switching process, so the switching time becomes shorter, as reported in Fig. 10. The dependence of the correction on the size of the structure is reported in Fig. 11, showing how the required correction is higher for larger surface

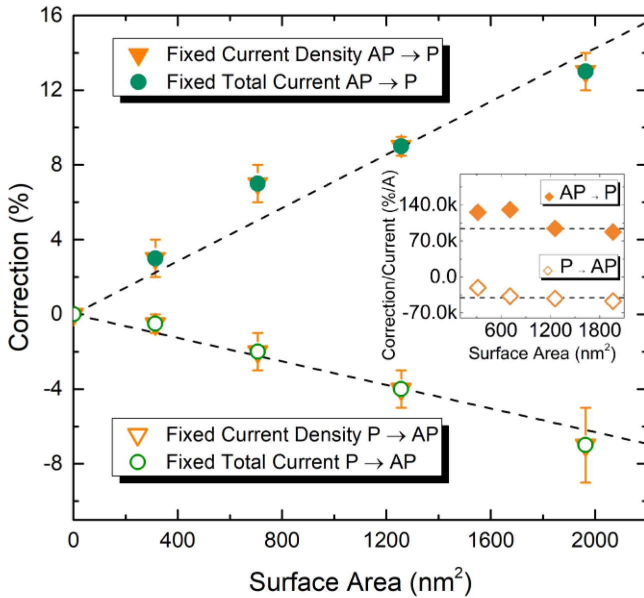

FIGURE 11. Dependence of the current correction on the surface area of the structure at $T = 300$ K, for both P → AP and AP → P switching. The dashed lines represent a linear fit. In the inset, the ratio of correction over total current is shown for every surface area.

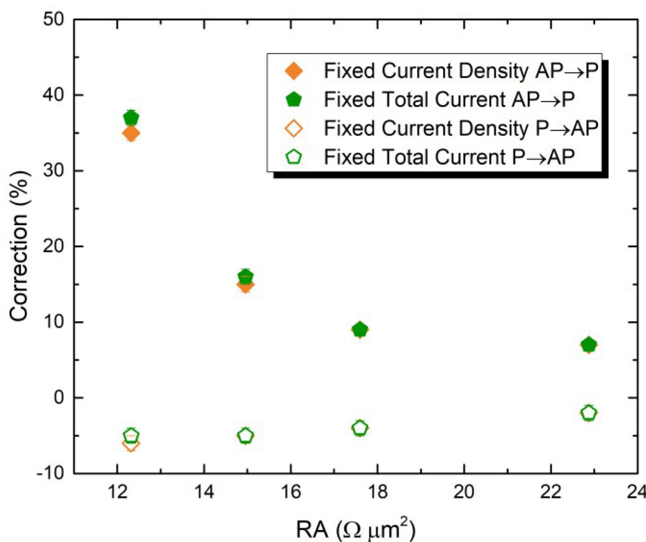

FIGURE 12. Dependence of the current correction on the resistance area of the structure at $T = 300$ K, for both P → AP and AP → P switching.

areas. The inset shows that the ratio of the correction on the current value does not depend on the area, underlining how the correction increases with the total current.

Finally, Fig. 12 shows the dependence of the correction on the resistance area of the structure. At lower *RA* values, both the current and the current density increase, leading to much faster switching and high amount of correction required to reproduce the switching times of the fixed voltage approach.

The dependence of the correction on both the surface area and the resistance area agree with the previous discussion: when the switching time becomes shorter, the required correction increases. These findings will help in the development of a compact model for predicting the switching time of STT-MRAM devices using a simple expression for the current density.

IV. CONCLUSION

We compared the switching times obtained under the assumption of a fixed voltage across the structure to the results of two approximations of switching under fixed current density and fixed total current constraints. We showed that a correction of the fixed current values is required to correctly reproduce the switching time distribution in a broad TMR range. The current correction is not universal and depends on system parameters, such as TMR, temperature, and size. We performed simulations with a macrospin model and observed that the results can be explained by the dependence of the correction on the switching time, with a shorter switching time always requiring a larger correction. Understanding the behavior of the current correction allows for the simple constant current density approach to correctly reproduce the switching time distribution, so that it can be employed in place of more complex and time consuming approaches. The development of a compact model for the correction will thus allow to obtain fast simulation tools for aiding and guiding the design of future devices.

REFERENCES

[1] S. Aggarwal *et al.*, "Demonstration of a reliable 1 Gb standalone spin-transfer torque MRAM for industrial applications," in *Proc. IEEE Int. Electron Devices Meeting (IEDM) Conf.*, San Francisco, CA, USA, 2019, pp. 1–4, doi: 10.1109/IEDM19573.2019.8993516

[2] K. Lee *et al.*, "1Gbit high density embedded STT-MRAM in 28nm FDSOI technology," in *Proc. IEEE Int. Electron Devices Meeting (IEDM) Conf.*, San Francisco, CA, USA, 2019, pp. 1–4, doi: 10.1109/IEDM19573.2019.8993551.

[3] V. B. Naik *et al.*, "Manufacturable 22nm FD-SOI embedded MRAM technology for industrial-grade MCU and IOT applications," in *Proc. IEEE Int. Electron Devices Meeting (IEDM) Conf.*, San Francisco, CA, USA, 2019, pp. 1–4, doi: 10.1109/IEDM19573.2019.8993454.

[4] G. Hu *et al.*, "Spin-transfer torque MRAM with reliable 2 ns writing for last level cache applications," in *Proc. IEEE Int. Electron Devices Meeting (IEDM) Conf.*, San Francisco, CA, USA, 2019, pp. 1–4, doi: 10.1109/IEDM19573.2019.8993604.

[5] W. J. Gallagher *et al.*, "22nm STT-MRAM for reflow and automotive uses with high yield, reliability, and magnetic immunity and with performance and shielding options," in *Proc. IEEE Int. Electron Devices Meeting (IEDM) Conf.*, San Francisco, CA, USA, 2019, pp. 1–4, doi: 10.1109/IEDM19573.2019.8993469.

[6] S. Sakhare *et al.*, "Enablement of STT-MRAM as last level cache for the high performance computing domain at the 5nm node," in *Proc. IEEE Int. Electron Devices Meeting (IEDM) Conf.*, San Francisco, CA, USA, 2019, pp. 1–4, doi: 10.1109/IEDM.2018.8614637.

[7] J. G. Alzate *et al.*, "2 MB array-level demonstration of STT-MRAM process and performance towards L4 cache applications," in *Proc. IEEE Int. Electron Devices Meeting (IEDM) Conf.*, San Francisco, CA, USA, 2019, pp. 1–4, doi: 10.1109/IEDM19573.2019.8993474.

[8] J. C. Slonczewski, "Current-driven excitation of magnetic multilayers," *J. Magn. Magn. Mater.*, vol. 159, pp. L1–L7, Jun. 1996, doi: 10.1016/0304-8853(96)00062-5.

[9] L. Berger, "Emission of spin waves by a magnetic multilayer traversed by a current," *Phys. Rev. B, Condens. Matter*, vol. 54, pp. 9353–9358, Oct. 1996, doi: 10.1103/PhysRevB.54.9353.

[10] A. Makarov, "Modeling of emerging resistive switching based memory cells," Ph.D. dissertation, Dept. Inst. Microelectronics, Vienna Univ. Technol., Vienna, Austria, 2014, doi: 10.13140/RG.2.2.11456.74242.

[11] W. Skowronski *et al.*, "Understanding stability diagram of perpendicular magnetic tunnel junctions," *Sci. Rep.*, vol. 7, Aug. 2017, Art. no. 10172, doi: 10.1038/s41598-017-10706-2.

[12] S. Fiorentini, R. L. de Orio, S. Selberherr, J. Ender, W. Goes, and V. Sverdlov, "Perpendicular STT-MRAM switching at fixed voltage and at fixed current," in *Proc. 4th IEEE Electron Devices Technol. Manuf. Conf. (EDTM)*, Penang, Malaysia, 2020, pp. 1–4, doi: 10.1109/EDTM47692.2020.9117985.

[13] S. Ikeda *et al.*, "Tunnel magnetoresistance of 604% at 300 K by suppression of Ta diffusion in CoFeB/MgO/CoFeB pseudo-spin-valves annealed at high temperature," *Appl. Phys. Lett.*, vol. 93, Aug. 2008, Art. no. 082508, doi: 10.1063/1.2976435.

[14] A. Makarov, T. Windbacher, V. Sverdlov, and S. Selberherr, "CMOS-compatible spintronic devices: A review," *Semicond. Sci. Technol.*, vol. 31, Oct. 2016, Art. no. 113006, doi: 10.1088/0268-1242/31/11/113006.

[15] S. Bhatti, R. Sbiaa, A. Hirohata, H. Ohno, S. Fukami, and S. N. Piramanayagam, "Spintronics based random access memory: A review," *Mat.Today*, vol. 20, pp. 530–548, Nov. 2017, doi: 10.1016/j.mattod.2017.07.007.

[16] J. C. Slonczewski, "Currents, torques, and polarization factors in magnetic tunnel junctions," *Phys. Rev. B*, vol. 71, Jan. 2005, Art. no. 024411, doi: 10.1103/PhysRevB.71.024411.

[17] D. Aurelio, L. Torres, and G. Finocchio, "Magnetization switching driven by spin-transfer-torque in high-TMR magnetic tunnel junctions," *J. Magn. Magn. Mat.*, vol. 321, pp. 3913–3920, Dec. 2009, doi: 10.1016/j.jmmm.2009.07.050.

[18] H. Sato *et al.*, "CoFeB thickness dependence of thermal stability factor in CoFeB/MgO perpendicular magnetic tunnel junctions," *IEEE Mag. Lett.*, vol. 3, Apr. 2012, Art. no. 3000204, doi: 10.1109/LMAG.2012.2190722.

[19] H. Sato, M. Yamanouchi, S. Ikeda, S. Fukam, F. Matsukura, and H. Ohno, "MgO/CoFeB/Ta/CoFeB/MgO recording structure in magnetic tunnel junctions with perpendicular easy axis," *IEEE Trans. Mag.*, vol. 49, no. 7, pp. 4437–4440, Jul. 2013, doi: 10.1109/TMAG.2013.2251326.

[20] S. Fiorentini, R. Orio, W. Goes, J. Ender, and V. Sverdlov, "Comprehensive comparison of switching models for perpendicular spin-transfer torque MRAM cells," in *Proc. Int. Conf. Simulat. Semicond. Process. Devices (SISPAD)*, Udine, Italy, 2019, pp. 57–60, doi: 10.1109/SISPAD.2019.8870359.